CTEQ distributions with intrinsic charm

Marco Guzzi

On behalf of the CTEQ-TEA collaboration

MANCHESTER 1824
The University of Manchester

CTEQ

Deep Inelastic scattering and related subjects
Birmingham, UK, 3-7 April 2017

DIS17

Problem

the charm PDF in most of the QCD global analyses of world data is calculated and not fitted, with boundary condition for DGLAP evolution calculated perturbatively (matching condition when switching from nf=3 to nf=4 flavours)
$c(x,Q=mc) = 0$

is this sufficient?

is there a (sizable) non-perturbative contribution to charm PDF?

What physics effects can lead to a non-zero fitted c(x, Q=mc)?

PDF fits may include a ``fitted charm'' PDF

``Fitted charm'' = ``nonperturbative charm''

+ other (possibly not universal)

higher O(αs) / Higher power terms

The perturbative charm PDF component cancels near the threshold up to a higher order

The 'fitted charm component' may approximate for a missing higher-order term or a power-suppressed component of a 'sea-like'or 'valence-like' type

Sea-like and valence-like PDFs

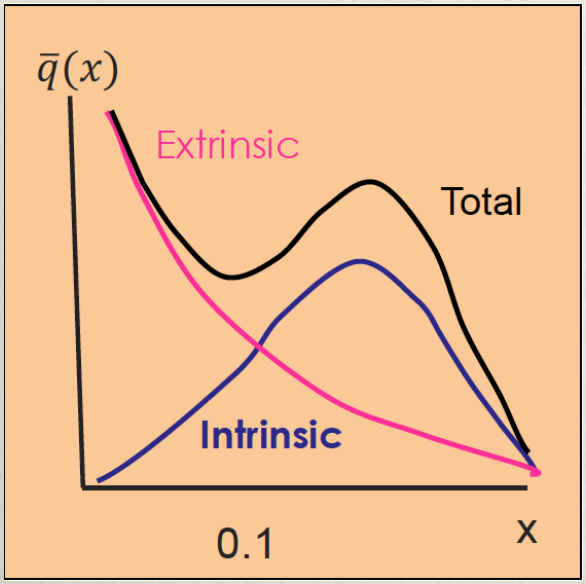

A simple model for a quark PDF at Q0 consists of two components:

1. Sea-like ("extrinsic") component:

- monotonic in *x*, satisfies

$$q(x) \propto x^{-1} \quad x \to 0$$

  - may be generated in several ways, e.g.,
    - in perturbative QCD from gluon splittings

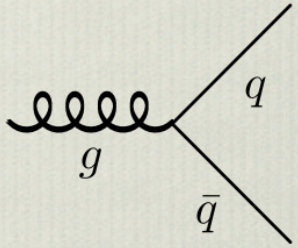

    - in lattice QCD from disconnected diagrams

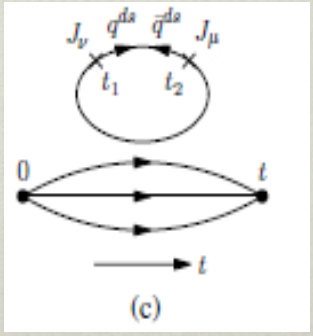

Sea-like and valence-like PDFs

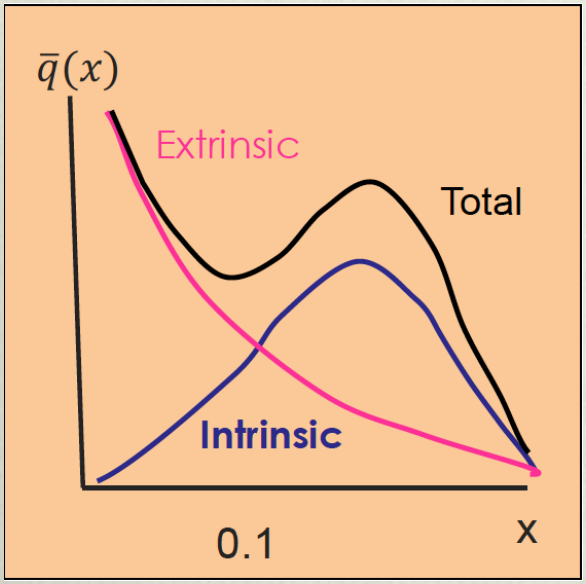

A simple model for a quark PDF at Q0 consits of two components:

2. Valence-like ("intrinsic") component
peaks in *x*, satisfies

$$q(x) \propto x^{-1/2} \quad x \to 0$$

- may be generated in several ways, e.g.,
  - for all flavors, nonperturbatively from a uudQQbar Fock state:

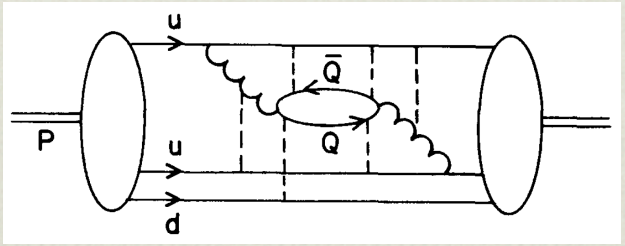

Brodsky, Peterson, Sakai, PRD 1981

- for ubar and dbar, in lattice QCD from connected diagrams

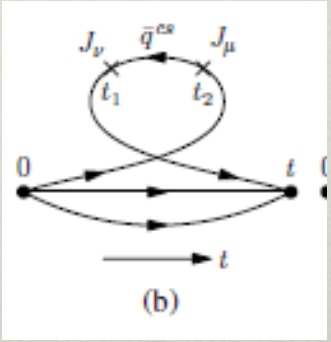

ubar and dbar PDFs, deconstruction

Smooth ubar+dbar parametrizations can hide existence of two components

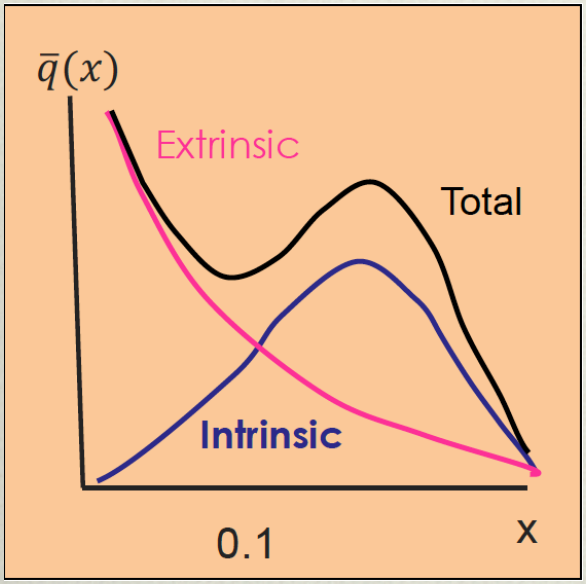

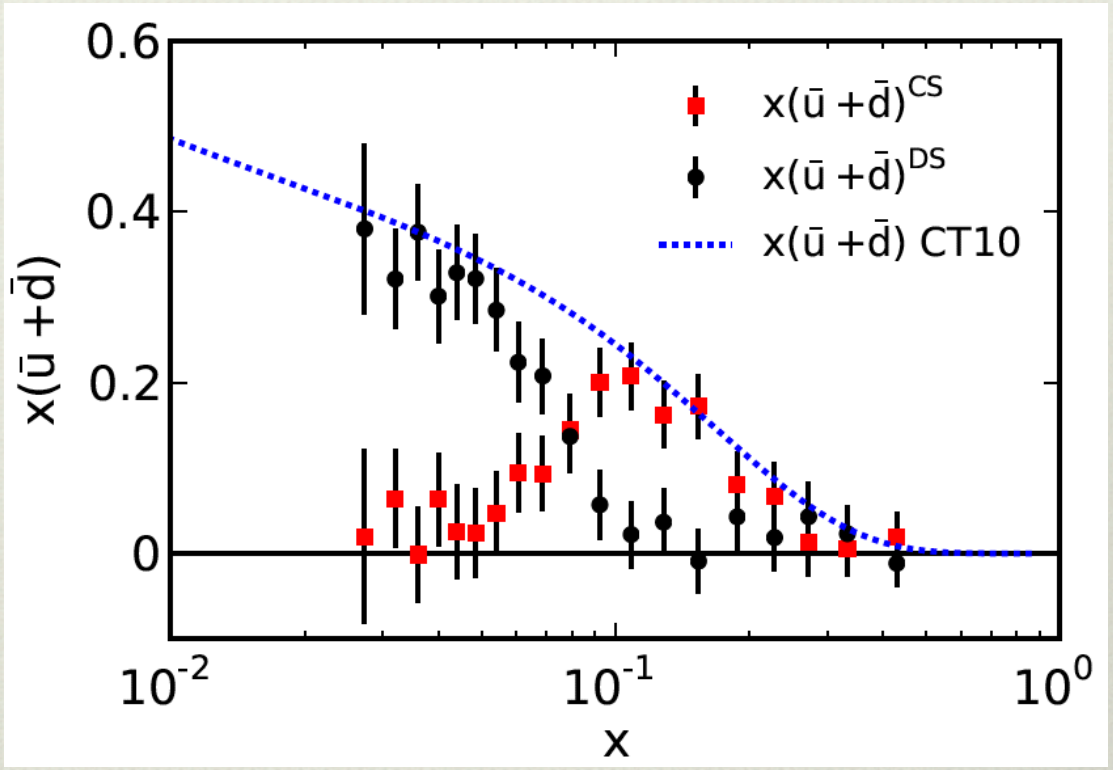

$$x(\bar{u}+\bar{d})^{CS}$$

$$x(\bar{u}+\bar{d})^{DS}$$

CS (connected Sea) and DS (Disconnected Sea) are related to intrinsic and extrinsic components respectively according to the short-distance expansion of the hadronic tensor in lattice QCD.

Liu, Chang, Cheng, Peng, PRL(2012) 1206.4339

Brodsky-Hoyer-Peterson-Sakai model: valence-like PDF from kinematic dependence

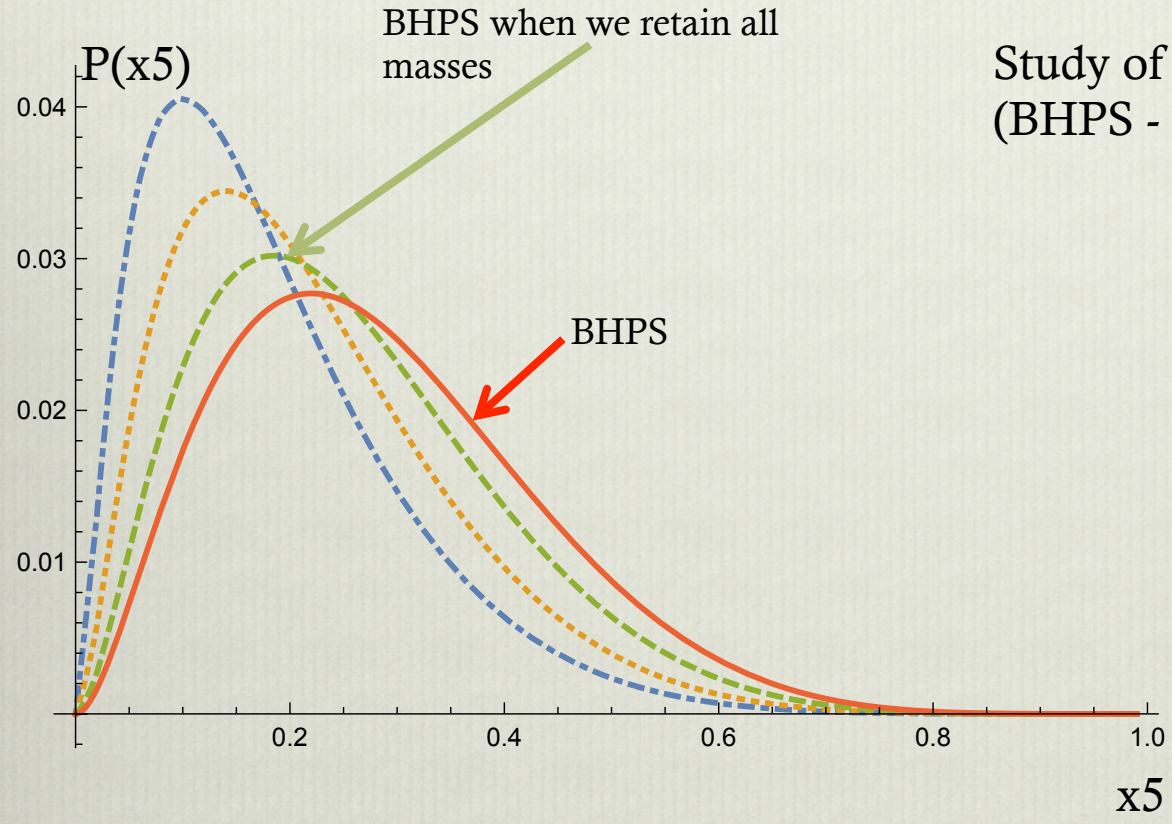

Study of the shapes assuming $\mathcal{P}_5^{Q\bar{Q}} = 0.01$
(BHPS - Brodsky et al, PLB 1980)

uud(uub), $m_u(\mu=2\text{GeV})=0.23$ GeV
uud(ddb), $m_d(\mu=2\text{GeV})=0.47$ GeV
uud(ccb), $m_c(\mu=2\text{GeV})=1.27$ GeV
BHPS

Kinematic conditions for BHPS charm also explored analytically by J. Bluemlein in PLB2016

Mp=1 GeV

$$P(x_5) = \int_0^1 dx_1 \dots dx_4 \delta(1 - \sum_{i=1}^{5} x_i) \frac{1}{\left[M_p^2 - \sum_{i=1}^{5} \frac{m_i^2}{x_i}\right]^2}$$

x-dependence distribution for intrinsic charm in the BHPS model with all masses kept

PDF fits may include a ``fitted charm'' PDF

``Fitted charm'' = ``intrinsic charm''

+ other (possibly not universal)

higher O(αs) / Higher power terms

We don't have an agreed definition/framework to factorize intrinsic charm contributions.

DIS HQ factorization by Collins PRD(1998) was proved only for radiative charm

IC is a correction that scales like $\frac{\Lambda^2_{QCD}}{m_c^2} \ln\left(\frac{Q^2}{\mu^2}\right)$

There is no consensus on how to factorize these contributions in DIS

But assuming that factorization exists for IC we can perform phenomenological studies to estimate the impact of IC on the CT14 global analysis of PDFs at NNLO.

Three types of charm content in the proton

1. Perturbative charm CT14:

$$c(x, Q_0) = 0 \quad \text{at} \quad \mu = \mathrm{Q_0} = \mathrm{m_c}$$

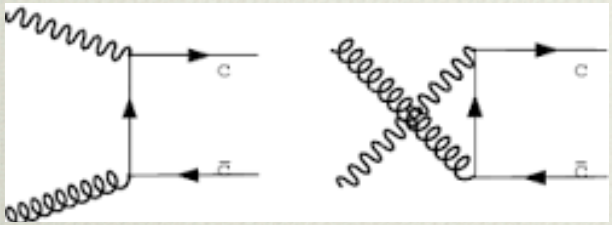

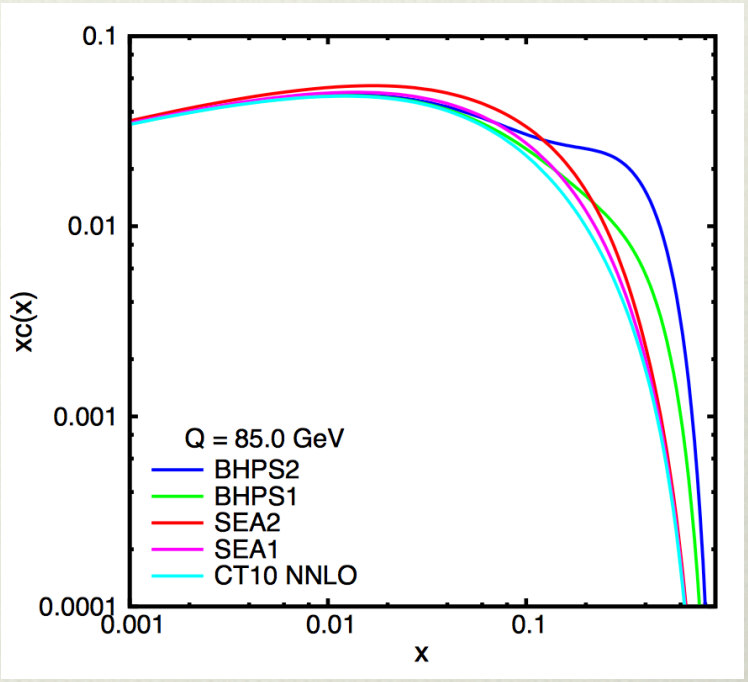

2. Intrinsic ``valence like'' charm:

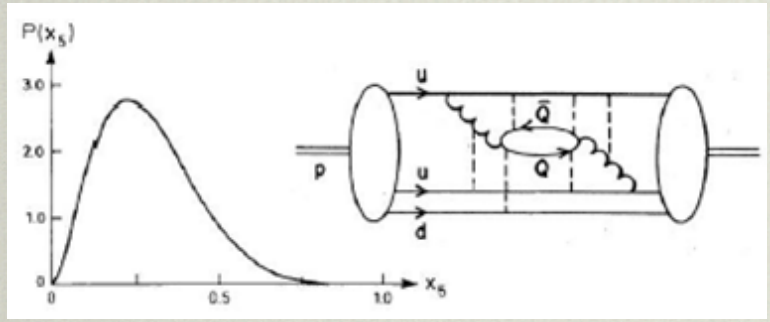

Light cone models BHPS (Brodsky et al 1980)
(see also 1504.06287 by Brodsky, Kusina, Lyonnet, Schienbein, Spiesberger, Vogt)

3. ``sea like'' charm:
a purely phenomenological scenario in which the shape of the charm distribution is sea-like—i.e., similar to that of the light flavor sea quarks, except for an overall mass-suppression.

Parametrizations for BHPS and SEA models

- "Valence-like" charm quark PDF according to the BHPS model (scale is unknown in this model):

Brodsky et al PLB 1980

$$c(x) = \bar{c}(x) = \frac{1}{2} A x^2 \left[\frac{1}{3}(1-x)\,(1+10x+x^2) - 2x(1+x)\ln(1/x) \right]$$

- "BHPS3 model: we include intrinsic uubar, ddbar and ccbar with numeric solutions for the BHPS model.

- ``Sea-like'' charm quark distribution, similar to that of the light flavor sea quarks:

$$c(x) = \bar{c}(x) = A\left[\bar{d}(x, Q_0) + \bar{u}(x, Q_0)\right]$$

❖ We characterize the magnitude of IC by the momentum fraction carried by **charm at starting scale Q0=1.3 GeV**:

$$\langle x \rangle_{c+\bar{c}} = \int_0^1 x \left[c(x) + \bar{c}(x) \right] dx$$

SET UP FOR THE GLOBAL ANALYSIS for CT14 and CT14HERA2:
We mainly focus on the CT14 analysis, CT14HERA2 gives similar results

For all three models:

- α s(MZ) = 0.118, compatible with the world average value α s(MZ) = 0.1184±0.0007, and the standard for recent CT PDF fits.

- HOPPET - evolution code used to include nonperturbative charm models with NNLO matching, and to evolve the PDFs at NNLO.

- S-ACOT-χ NNLO --- CT GMVFN default scheme for heavy-flavour treatment in the inclusive DIS structure functions.
  Differences between ACOT-χ vs S-ACOT-χ for IC contr. are $\mathcal{O}\left(\Lambda^2/Q^2\right)$

- Production threshold kinematics are accounted for by using the χ convention. The other partons are parametrized at an initial scale Q0 = 1.295 GeV, as in the CT14 analysis.

- The charm-quark mass, mc = 1.3 GeV, is in the pole mass scheme unless otherwise specified.

Best fit for different IC choices

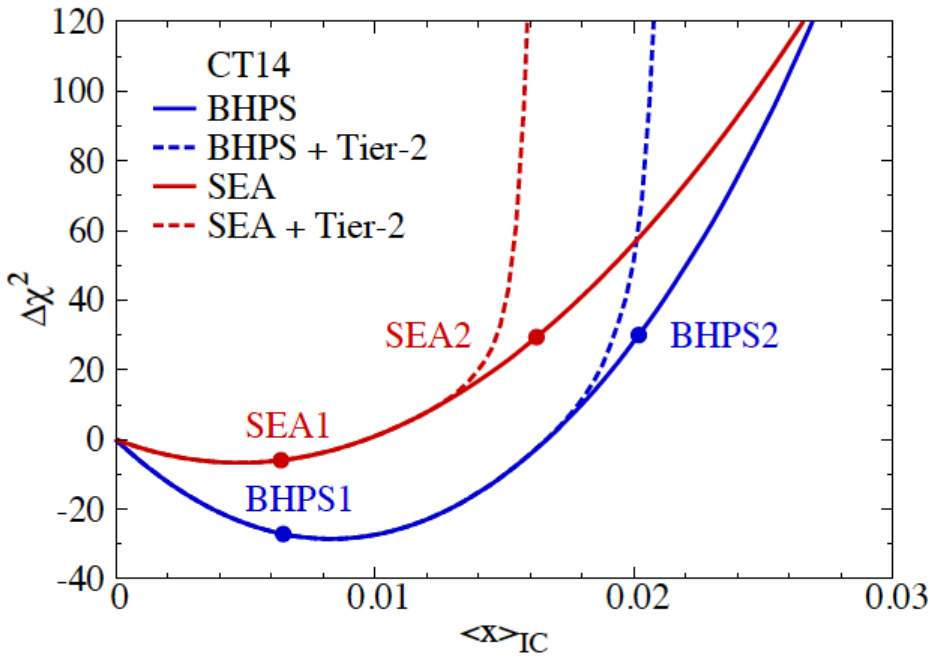

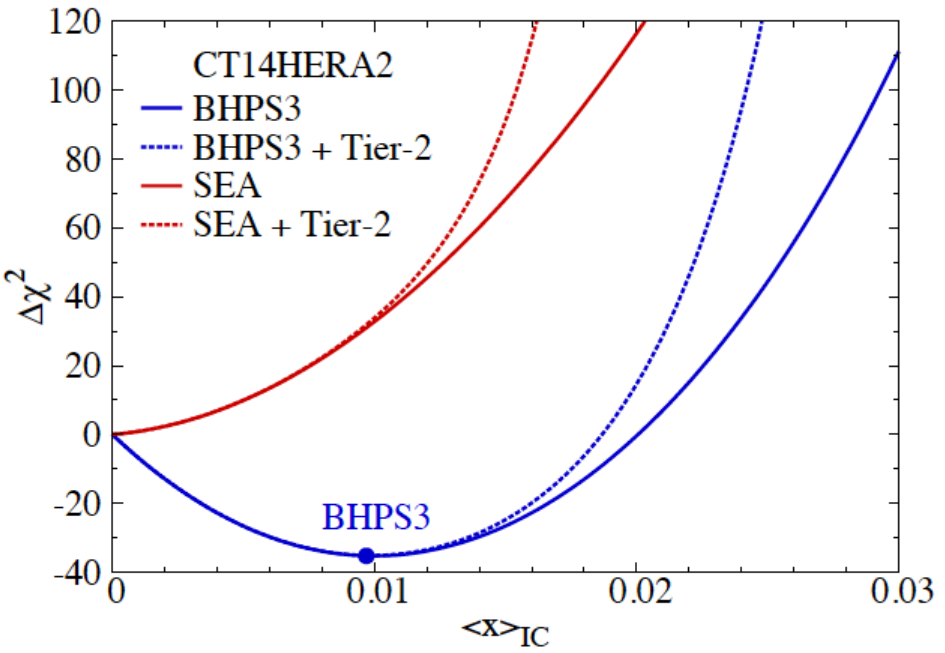

The dotted curves show $\Delta\chi^2 + T_2$ versus $\langle x \rangle_{\rm IC}$ for the two models of IC.

New upper limits on <x>IC for CT14 and CT14HERA2 at the 90% C.L.

$$\langle x \rangle_{\rm IC} \lesssim 0.021 \quad \text{BHPS for CT14,}$$
$$\langle x \rangle_{\rm IC} \lesssim 0.024 \quad \text{BHPS for CT14HERA2,}$$
$$\langle x \rangle_{\rm IC} \lesssim 0.016 \quad \text{SEA for CT14 and CT14HERA2.}$$

Impact of IC on the PDFs and their ratios

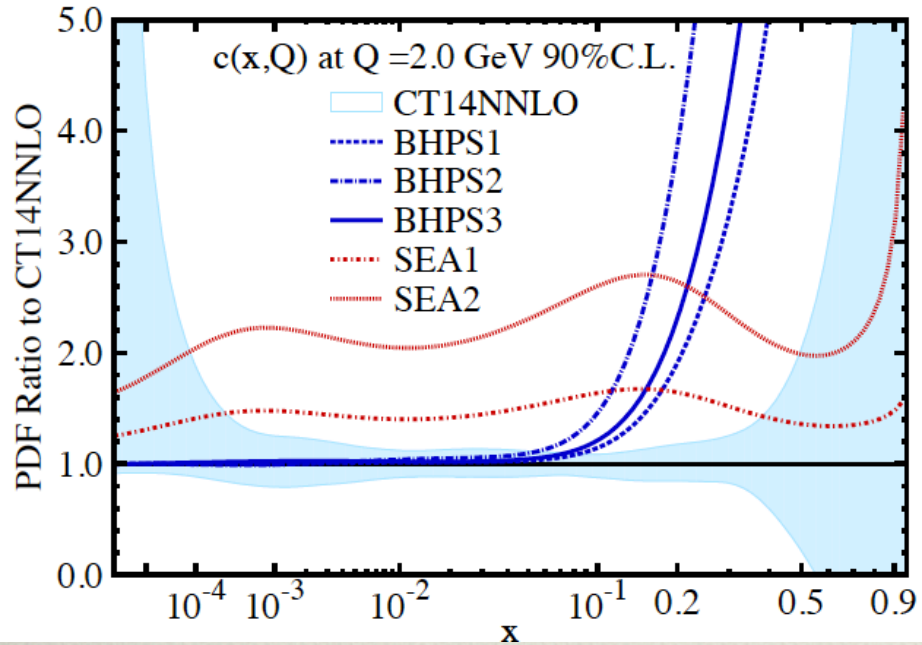

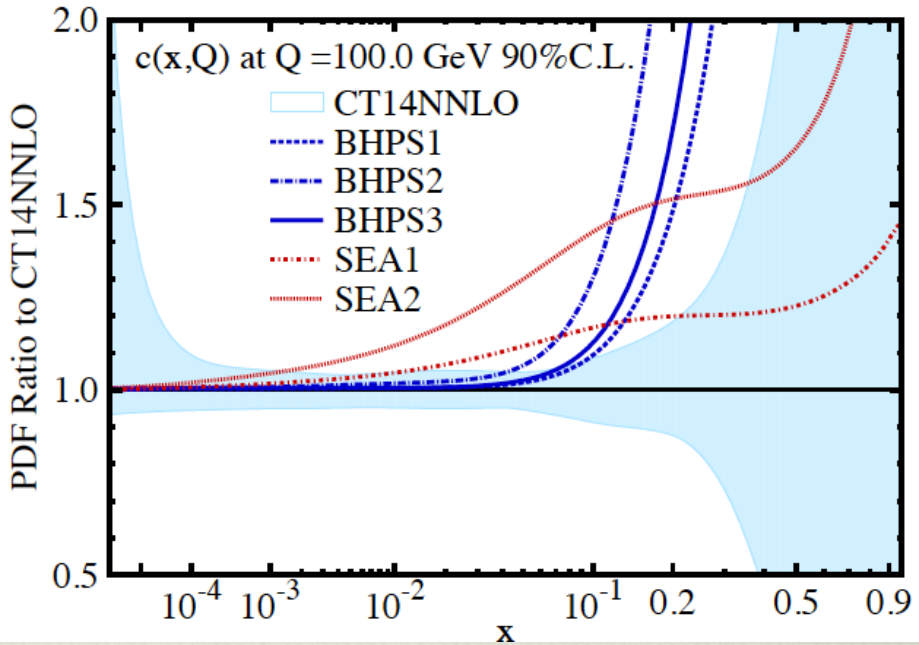

Study of Rc =(c+cbar)/(ubar+dbar) suppression ratio

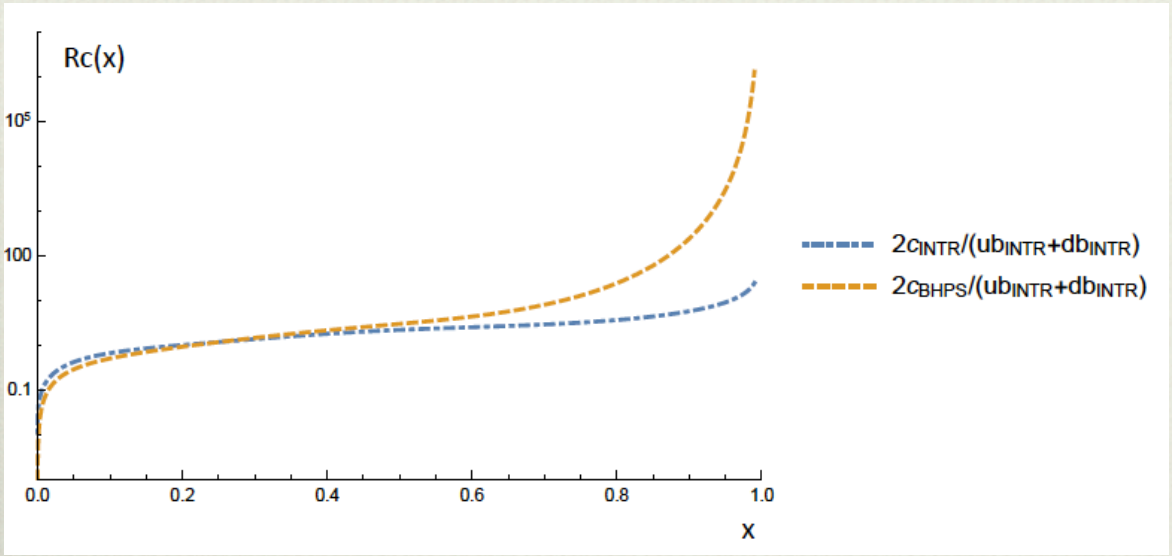

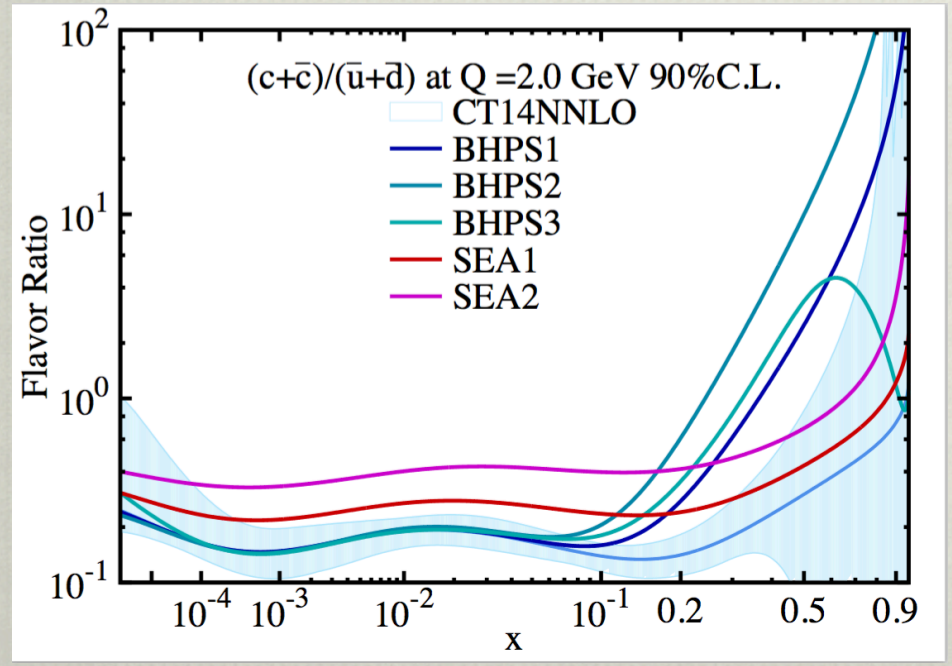

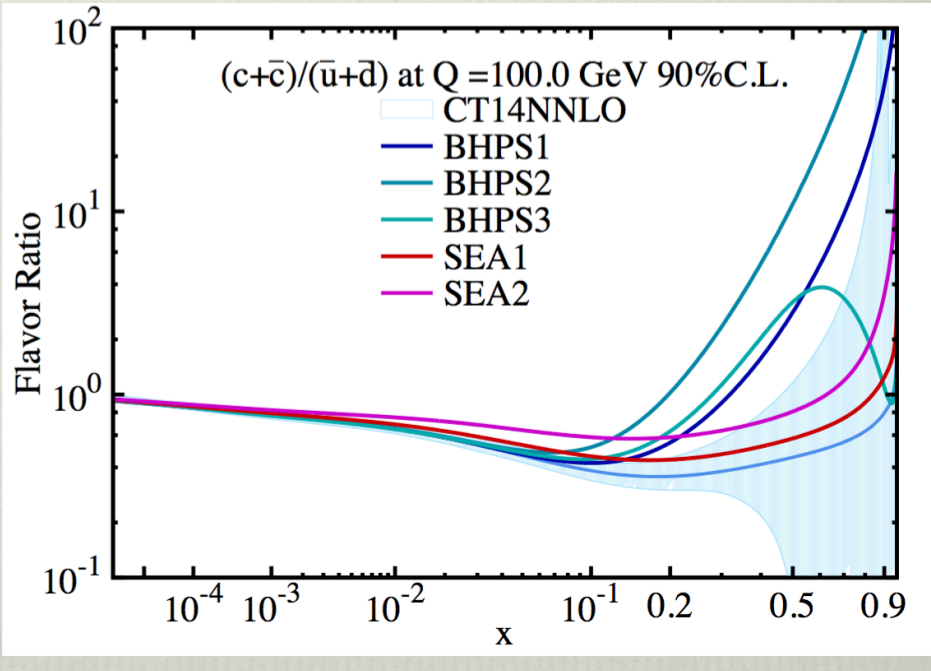

Impact of IC on luminosities

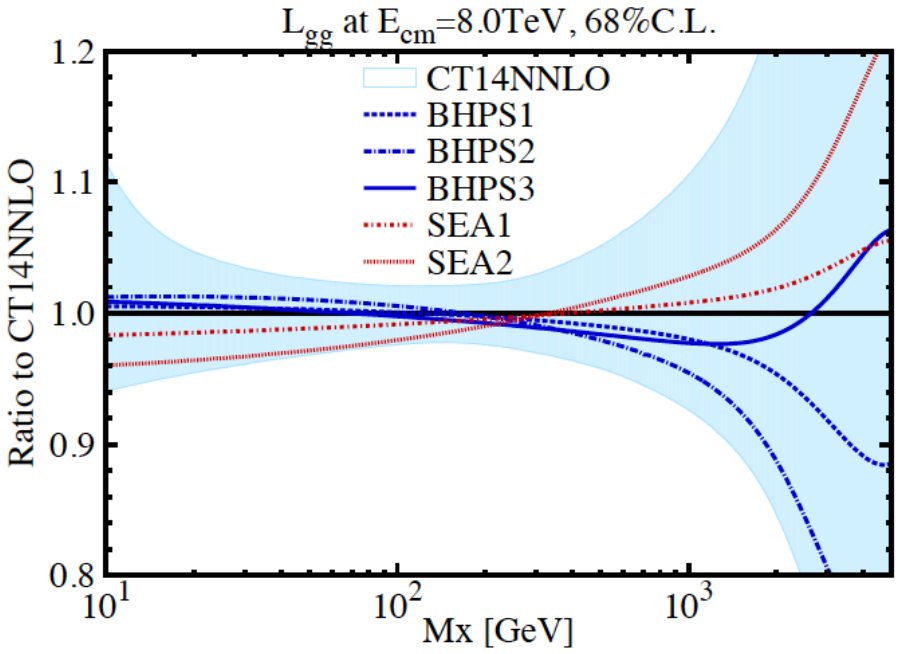

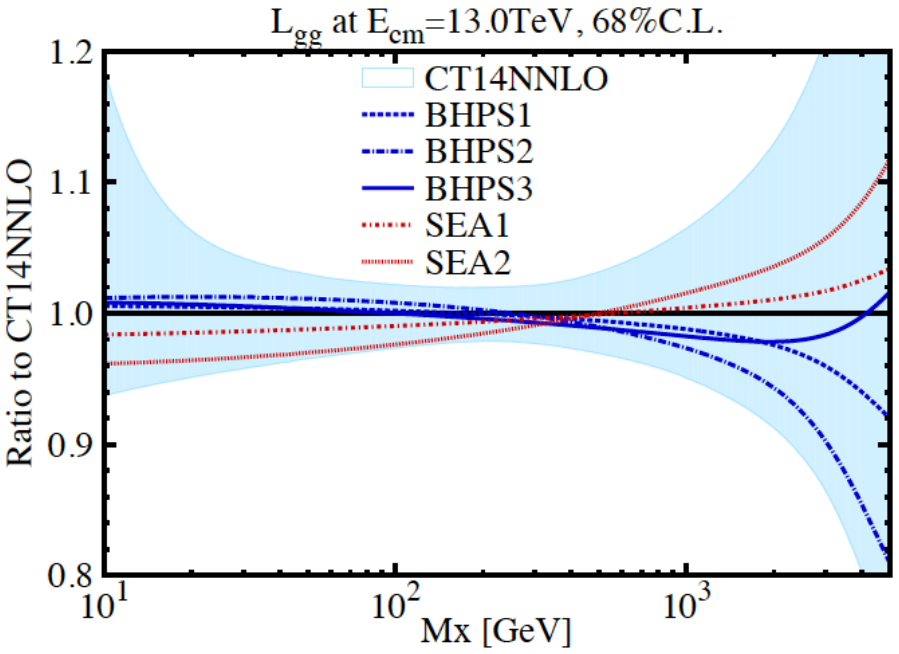

At √s = 8 TeV the most prominent distortions are from the SEA2 model which is suppressed at lower MX and is notably larger than CT14 for MX in the TeV range.
The BHPS models are almost coincident with CT14 for MX < 200 GeV: BHPS1 and BHPS2 are highly suppressed above MX > 300 GeV, while BHPS3 is suppressed for 0.3 <MX < 3 TeV and enhanced above this energy by approximately 3%.
The impact on the Higgs cross section is small, with sizable impacts on the high mass gg PDF luminosities, but still within uncertainties.

Impact from data: analysis using an effective gaussian χ^2 variable

-1<Sn<1 reasonable fit, i.e. within the errors; Sn > 3 poor fit.
Sn < −3 better than one would expect from normal statistical analysis

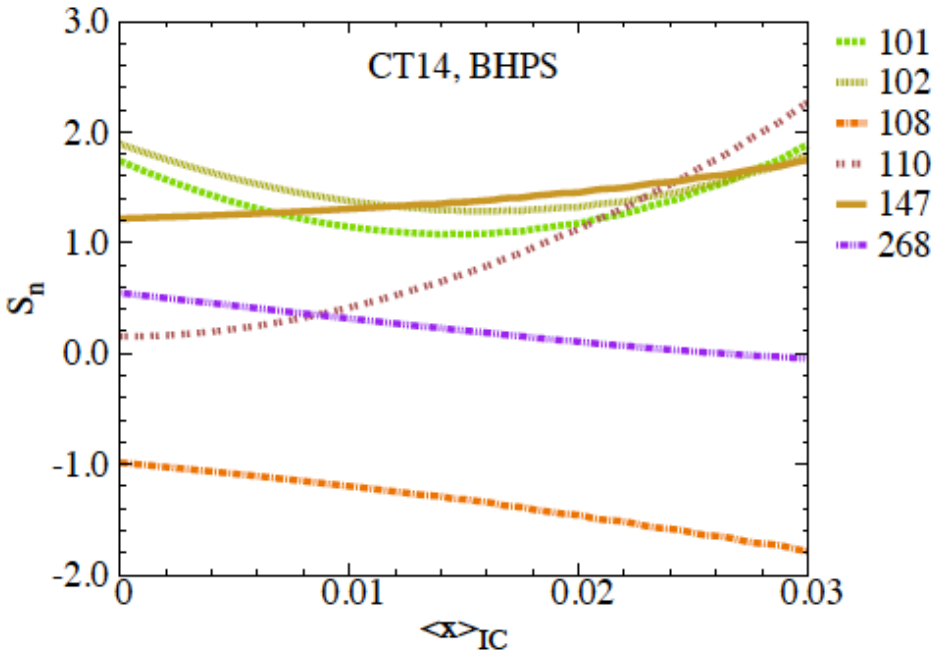

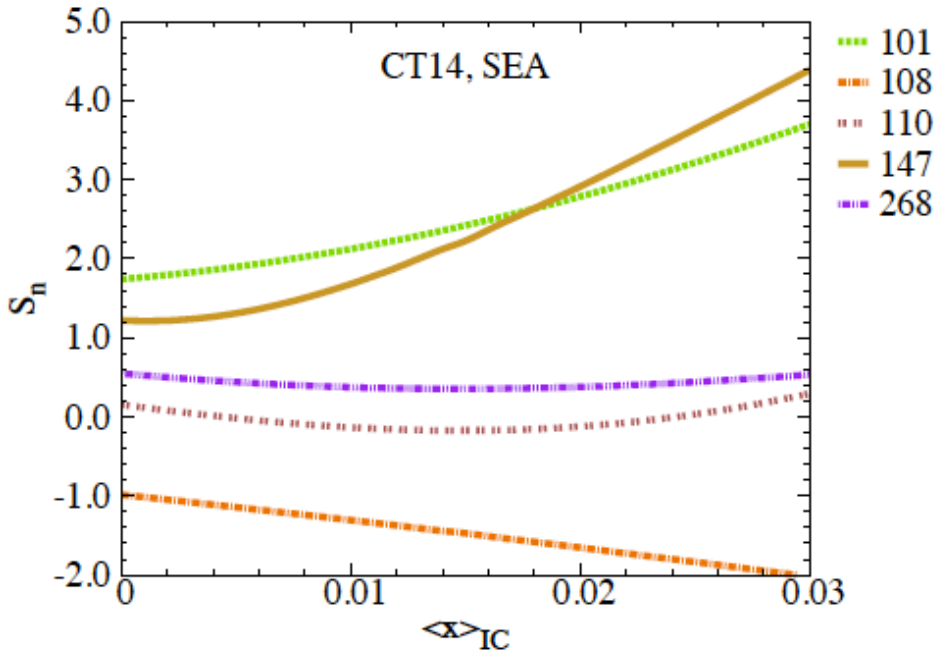

The CCFR structure function data (ID 110) is most sensitive to the BHPS model. And thus the upper limit on the $\langle x \rangle_{\mathrm{IC}}$ value for BHPS model comes from the CCFR structure function data.

The HERA combined charm data (ID 147) is most sensitive to the SEA model. Which means the HERA combined charm data sets the upper limit on $\langle x \rangle_{\mathrm{IC}}$ for the SEA model.

DEPENDENCE OF FIT ON THE CHARM-QUARK MASS

The combined HERA charm production and inclusive DIS data play an important role in the description of the goodness of fit. mc is a key input scale.

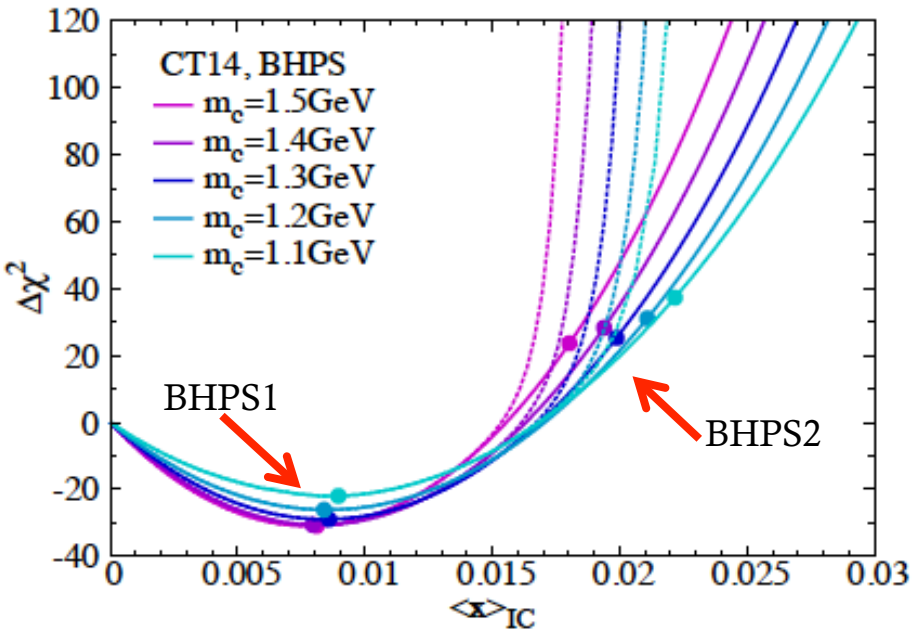

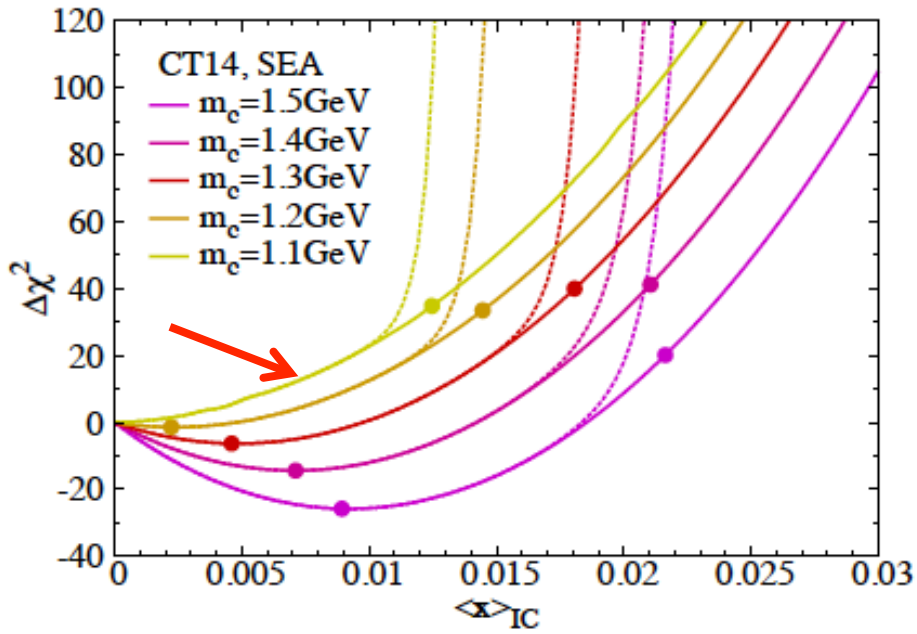

BHPS model: the position of the χ^2 minimum is relatively stable as mc is varied, while the upper limit on the amount of IC decreases to 1.7%. BHPS model is not dramatically affected by variations of mc

SEA model: limits on the amount of IC allowable are shifted towards higher values. ubar and dbar are well constrained by data (vector boson production in pp and pbar p) in the intermediate/small x region, and cannot change too much

In-depth study of CT14 IC fits (T.-J. Hou)

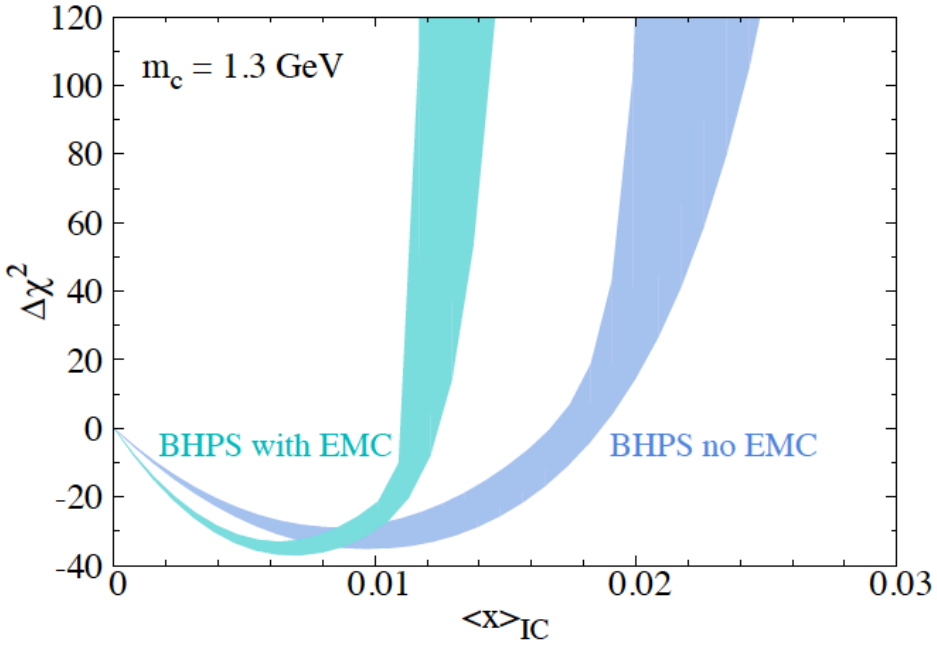

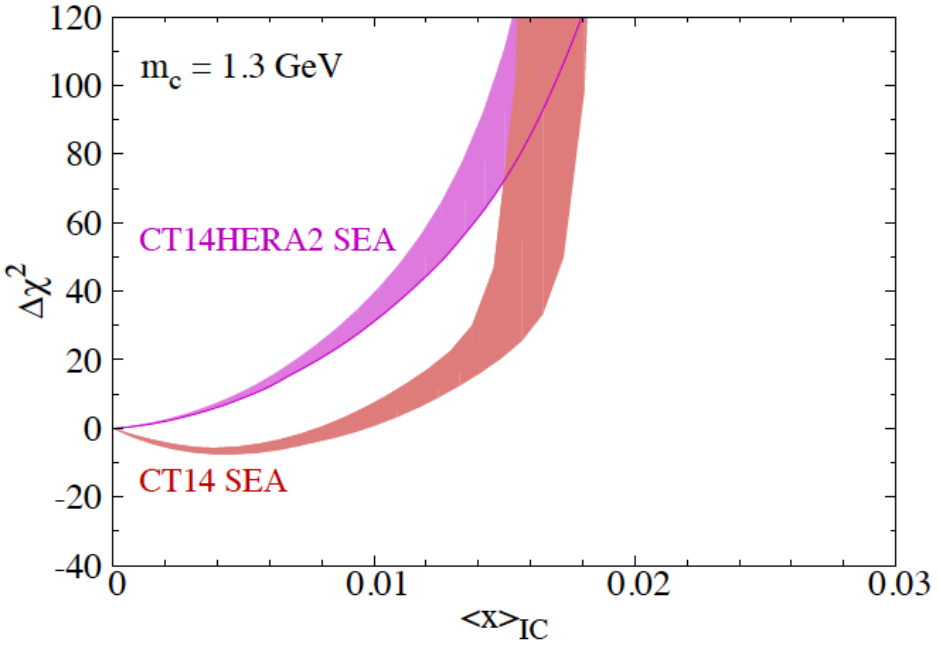

χ^2 as function of $\langle x \rangle_{\rm IC}$ in fits with and without the EMC data for both the BHPS and SEA models for mc = 1.3 GeV. For the BHPS model (left), the two distinct behaviors are from fits with and without the EMC data. For the SEA model (right) the two distinct behaviors are from different parametrizations in the CT14 and CT14HERA2 fits.

χ^2 values for CT14 and CT14HERA2 fits with and without EMC data

Candidate NNLO PDF fits	$\chi^2/N_{\rm pts}$		
	All Experiments	HERA inc. DIS	HERA $c\bar{c}$ SIDIS
CT14 + EMC (weight=0), no IC	1.10	1.02	1.26
CT14 + EMC (weight=10), no IC	1.14	1.06	1.18
CT14 + EMC BHPS	1.11	1.02	1.25
CT14 + EMC SEA	1.12	1.02	1.28
CT14 HERA2 + EMC (weight=0), no IC	1.09	1.25	1.22
CT14 HERA2 + EMC (weight=10), no IC	1.12	1.28	1.16
CT14 HERA2 BHPS+EMC	1.09	1.25	1.22
CT14 HERA2 SEA+EMC	1.11	1.26	1.26

The EMC data (1983), do not satisfy the stringent criteria on systematic uncertainties required in more recent experimental analyses.
This is one of the reasons why these measurements are not included in CTEQ PDF analyses, whose policy is to include only data with trusted systematic errors. However, it is still useful to examine how the EMC measurements of the heavy-flavor F2c structure function could possibly affect the amount of IC.

LHC searches for intrinsic charm

Z+c NLO computation with various models, without (left) and with parton shower (right)

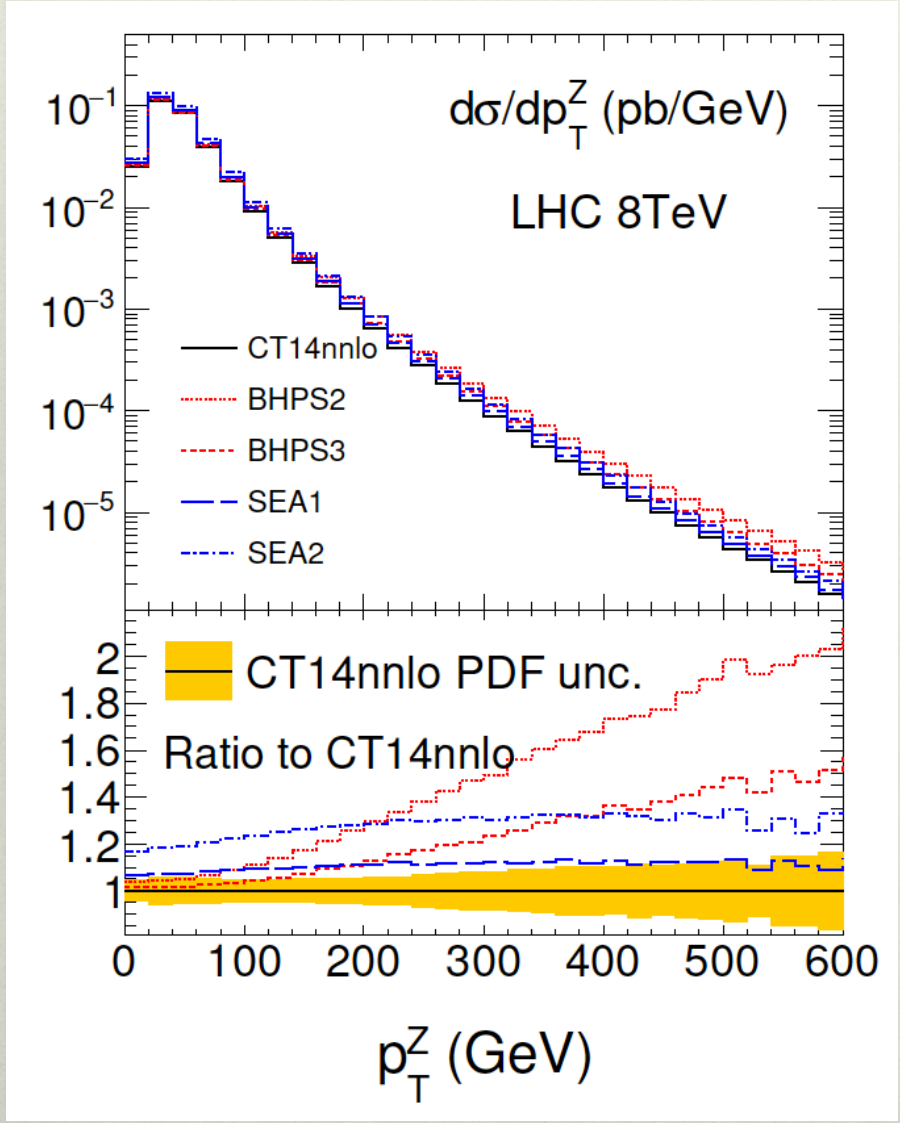

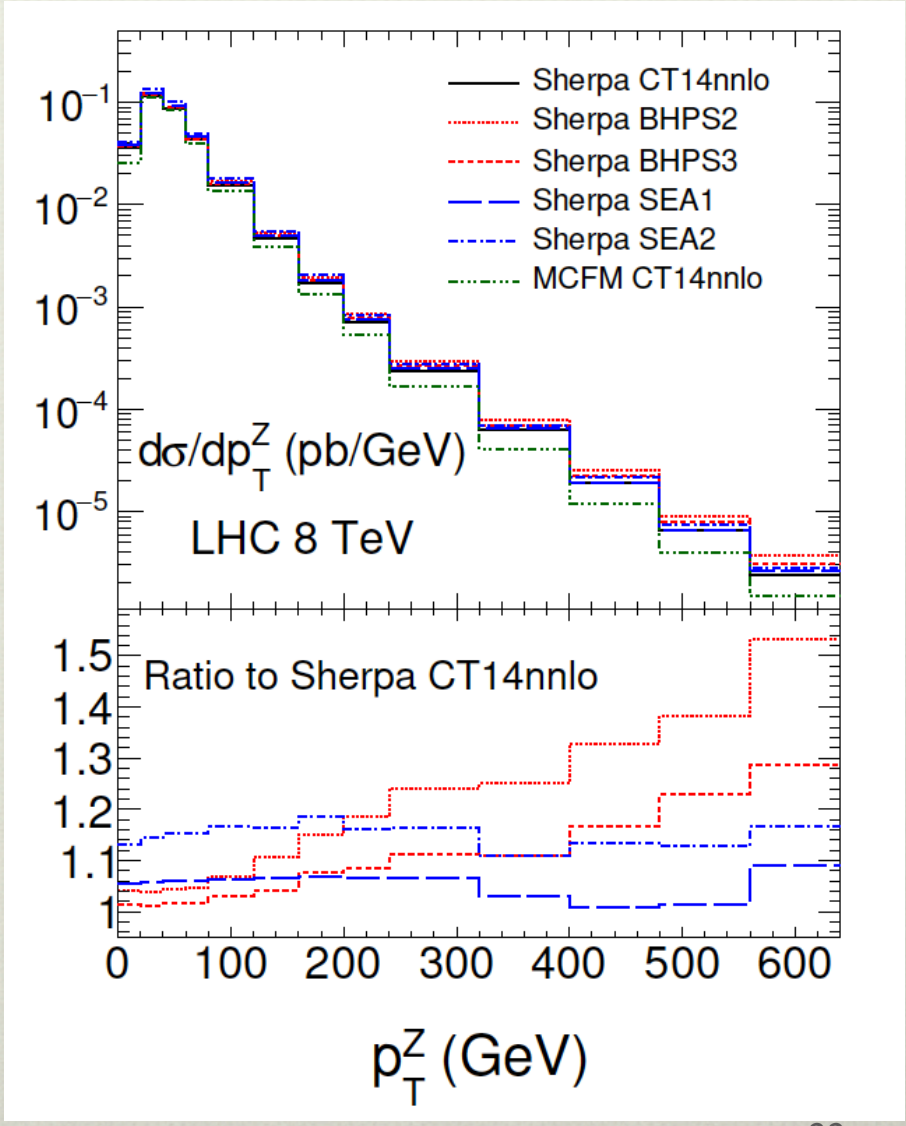

Z+c NLO LHC 13 TeV

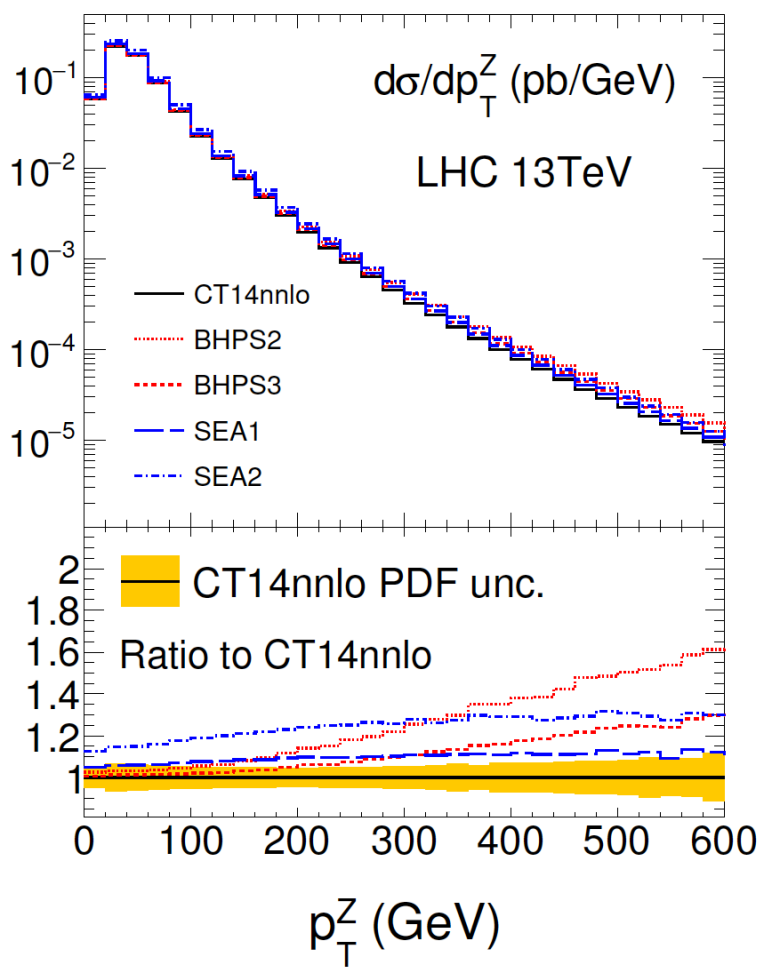

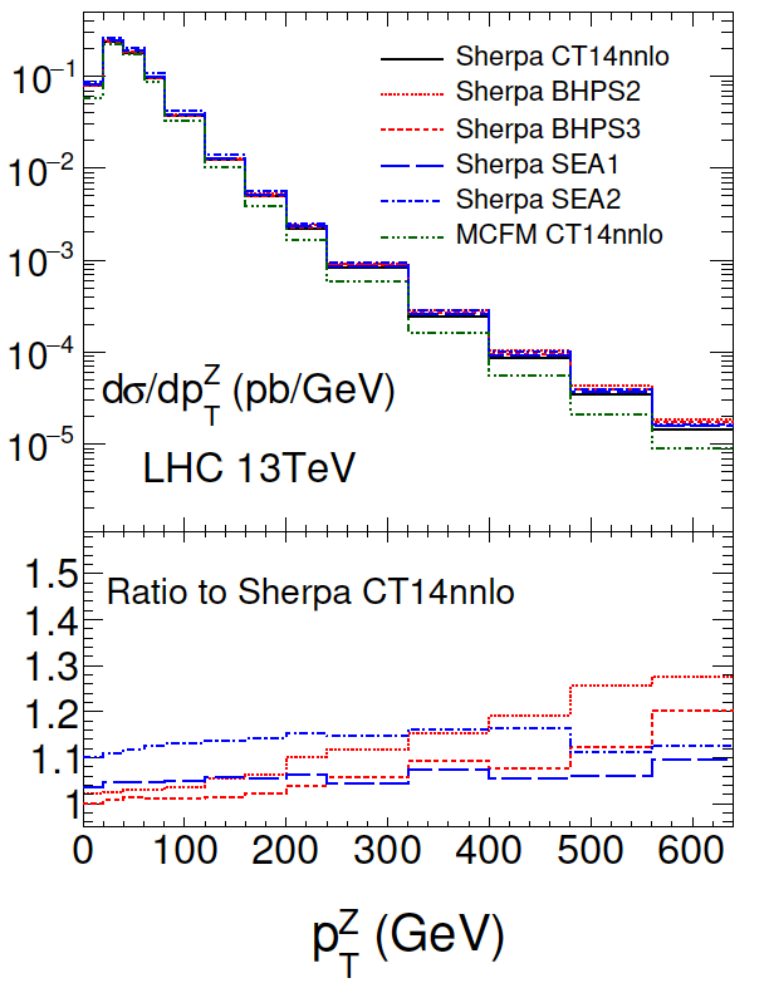

The parton shower has the most significant effect in dampening the hard pT(Z) tail especially for BHPS fits. Sherpa predictions include HO tree-level MEs compared to MCFM and therefore show enhancements in the harder pT(Z) region compared to MCFM. Similarly increasing or decreasing the number of multileg MEs in the merging changes the absolute level of pT.

Conclusions

- We explored the possibility of sizeable nonperturbative contribution to charm PDF **assuming that factorization for such contributions exists.**

- We have determined the magnitude of the IC component of the proton that is consistent with the CT14 global QCD analysis of hard scattering data: $\langle x \rangle < 2\%$ for BHPS IC and $\langle x \rangle < 1.6\%$ for SEA IC at 90% C.L..

- The allowed IC momentum fraction value increased for BHPS, and decreased for SEA model when we use CT14HERA2 set up.

- We analyzed the impact of EMC data: the allowed IC momentum fraction value decreases for BHPS model in fits with EMC data (but no control on systematic errors)

- We analyzed implication of IC in charm-sensitive processes at the LHC with parton shower: most significant effect in dampening the hard pT(Z) tail especially for BHPS fits.

- **Experimental confirmation still missing:** data from more sensitive measurements required; high energy and high luminosity fixed-target experiment needed. Constraining power of data still not sufficient.

BACKUP

Why this is important

If an intrinsic charm component (IC) is present at a low energy scale, it will participate fully in QCD dynamics and evolve along with the other partons as the energy scale increases:

- **observable consequences on physically interesting processes at high energies and short distances.**

- **Precision PDFs is required for precision determinations of key observables at the LHC sensitive to charm**

- **the c and cbar PDFs will be relevant to some important LHC measurements: production of W± and Z0 involves cd, cs, dc, sc and cc contributions.**

- **charmed particle production at the LHC, which will depend quite directly on the c and cbar partons**

- **Implications on New Physics Searches**

- **Important to understand the flavor content of the nucleon sea:**

- observation of the light-quark sea difference between db and ub in DIS and Drell-Yan
- extraction of strange quark content s+sb from semi-inclusive DIS
- lattice QCD calculations of sea quark contributions to nucleon orbital angular momenta.

CT14HERA2 ⇒ The CTEQ-TEA PDFs have been refitted NLO and NNLO by using the global CT14 data ensemble, but with the HERA2 measurements in place of HERA1.

Other changes w.r.t. CT14

CT14HERA2 global fit 3287 data points in total compared to 2947 in the original CT14:

1) The NMC muon-proton inclusive DIS data on F2p are dropped (cannot be fitted well; data is influenced by some unknown or underestimated systematic errors). We continue to include the NMC proton to deuteron ratio data on F2p /F2d.

2) The data table for the CMS 7 TeV 5 fb-1 inclusive jet experiment has been updated: no appreciable effects on the PDFs.

3) Introduction of 1 free parameter in the s(x,Q0) parametrization (Q0=1.3 GeV), in the end the number of eigenvector sets is 56 as in CT14.

$\chi^2_{\mathrm{CT14_{HERA2},NNLO}}/N_{pts} = 3596/3287 = 1.09$ $\chi^2_{\mathrm{CT14,NNLO}}/N_{pts} = 3250/2947 = 1.10$

CT14 Data sets ensemble I

ID#	Experimental data set	N_{pt}	χ^2_e	χ^2_e/N_{pt}	S_n
101	BCDMS F_2^p	337	384	1.14	1.74
102	BCDMS F_2^d	250	294	1.18	1.89
104	NMC F_2^d/F_2^p	123	133	1.08	0.68
106	NMC σ^p_{red}	201	372	1.85	6.89
108	CDHSW F_2^p	85	72	0.85	-0.99
109	CDHSW F_3^p	96	80	0.83	-1.18
110	CCFR F_2^p	69	70	1.02	0.15
111	CCFR xF_3^p	86	31	0.36	-5.73
124	NuTeV $\nu\mu\mu$ SIDIS	38	24	0.62	-1.83
125	NuTeV $\bar{\nu}\mu\mu$ SIDIS	33	39	1.18	0.78
126	CCFR $\nu\mu\mu$ SIDIS	40	29	0.72	-1.32
127	CCFR $\bar{\nu}\mu\mu$ SIDIS	38	20	0.53	-2.46
145	H1 σ_r^b	10	6.8	0.68	-0.67
147	Combined HERA charm production	47	59	1.26	1.22
159	HERA1 Combined NC and CC DIS	579	591	1.02	0.37
169	H1 F_L	9	17	1.92	1.7

Very important for PDF determination

CT14 Data sets ensemble II

ID#	Experimental data set	N_{pt}	χ^2_e	χ^2_e/N_{pt}	S_n
201	E605 Drell-Yan process	119	116	0.98	-0.15
203	E866 Drell-Yan process, $\sigma_{pd}/(2\sigma_{pp})$	15	13	0.87	-0.25
204	E866 Drell-Yan process, $Q^3 d^2\sigma_{pp}/(dQdx_F)$	184	252	1.37	3.19
225	CDF Run-1 electron A_{ch}, $p_{T\ell} > 25$ GeV	11	8.9	0.81	-0.32
227	CDF Run-2 electron A_{ch}, $p_{T\ell} > 25$ GeV	11	14	1.24	0.67
234	DØ Run-2 muon A_{ch}, $p_{T\ell} > 20$ GeV	9	8.3	0.92	-0.02
240	LHCb 7 TeV 35 pb^{-1} W/Z $d\sigma/dy_\ell$	14	9.9	0.71	-0.73
241	LHCb 7 TeV 35 pb^{-1} A_{ch}, $p_{T\ell} > 20$ GeV	5	5.3	1.06	0.30
260	DØ Run-2 Z rapidity	28	17	0.59	-1.71
261	CDF Run-2 Z rapidity	29	48	1.64	2.13
266	CMS 7 TeV 4.7 fb^{-1}, muon A_{ch}, $p_{T\ell} > 35$ GeV	11	12.1	1.10	0.37
267	CMS 7 TeV 840 pb^{-1}, elec. A_{ch}, $p_{T\ell} > 35$ GeV	11	10.1	0.92	-0.06
268	ATLAS 7 TeV 35 pb^{-1} W/Z cross sec., A_{ch}	41	51	1.25	1.11
281	DØ Run-2 9.7 fb^{-1} elec. A_{ch}, $p_{T\ell} > 25$ GeV	13	35	2.67	3.11
504	CDF Run-2 inclusive jet production	72	105	1.45	2.45
514	DØ Run-2 inclusive jet production	110	120	1.09	0.67
535	ATLAS 7 TeV 35 pb^{-1} incl. jet production	90	50	0.55	-3.59
538	CMS 7 TeV 5 fb^{-1} incl. jet production	133	177	1.33	2.51

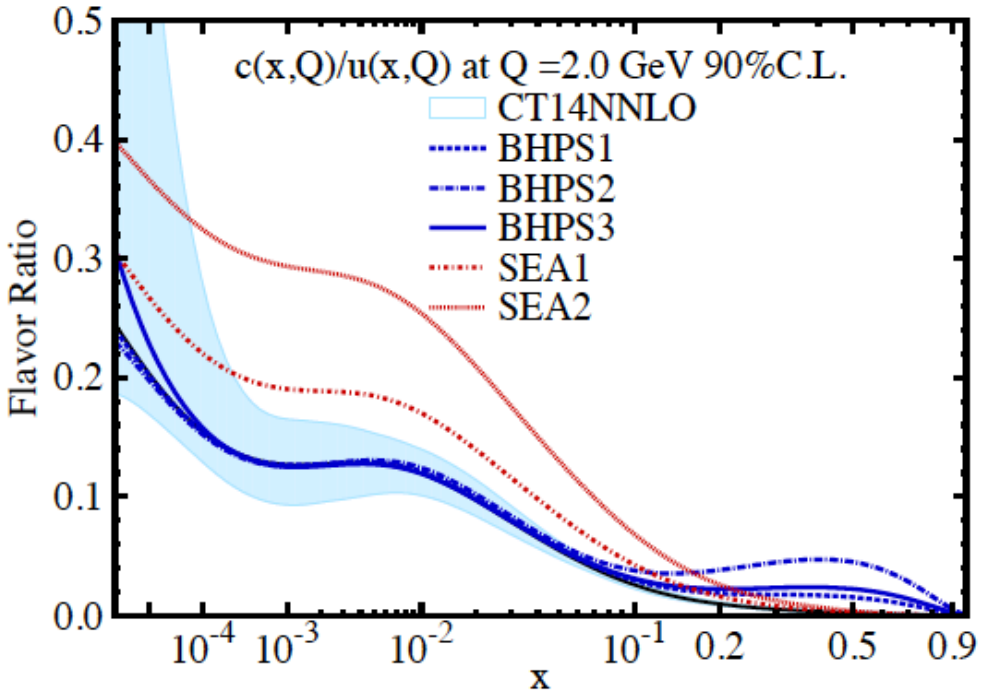
c(x,Q)/u(x,Q) at Q =2.0 GeV 90%C.L.
CT14NNLO
BHPS1
BHPS2
BHPS3
SEA1
SEA2
Flavor Ratio
0.0
0.1
0.2
0.3
0.4
0.5
10^{-4}
10^{-3}
10^{-2}
10^{-1}
0.2
0.5
0.9
x

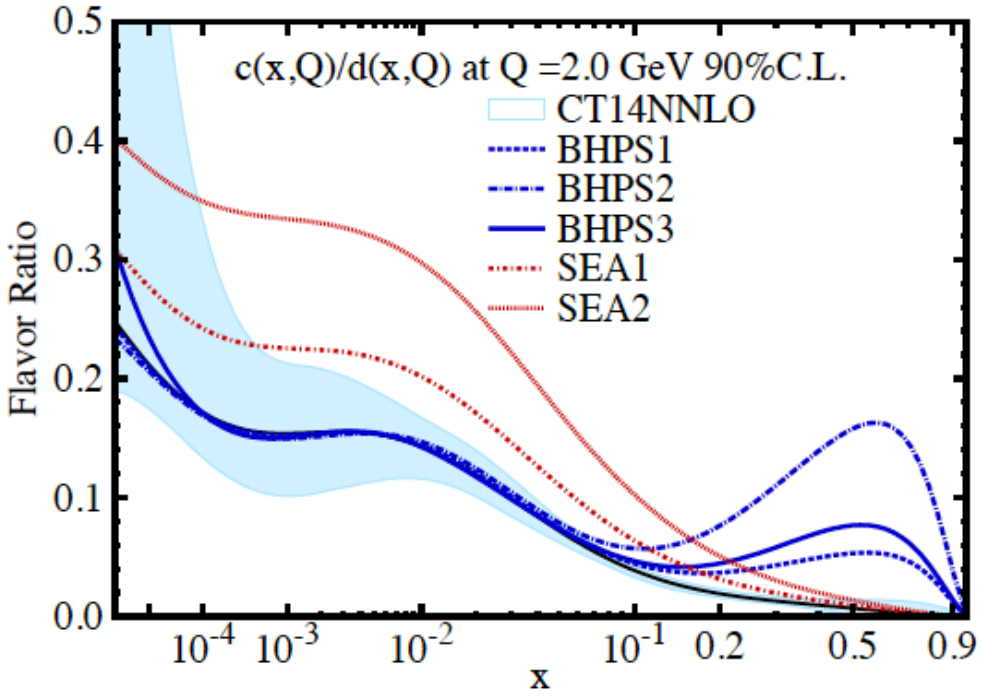
c(x,Q)/d(x,Q) at Q =2.0 GeV 90%C.L.
CT14NNLO
BHPS1
BHPS2
BHPS3
SEA1
SEA2
Flavor Ratio
0.0
0.1
0.2
0.3
0.4
0.5
10^{-4}
10^{-3}
10^{-2}
10^{-1}
0.2
0.5
0.9
x

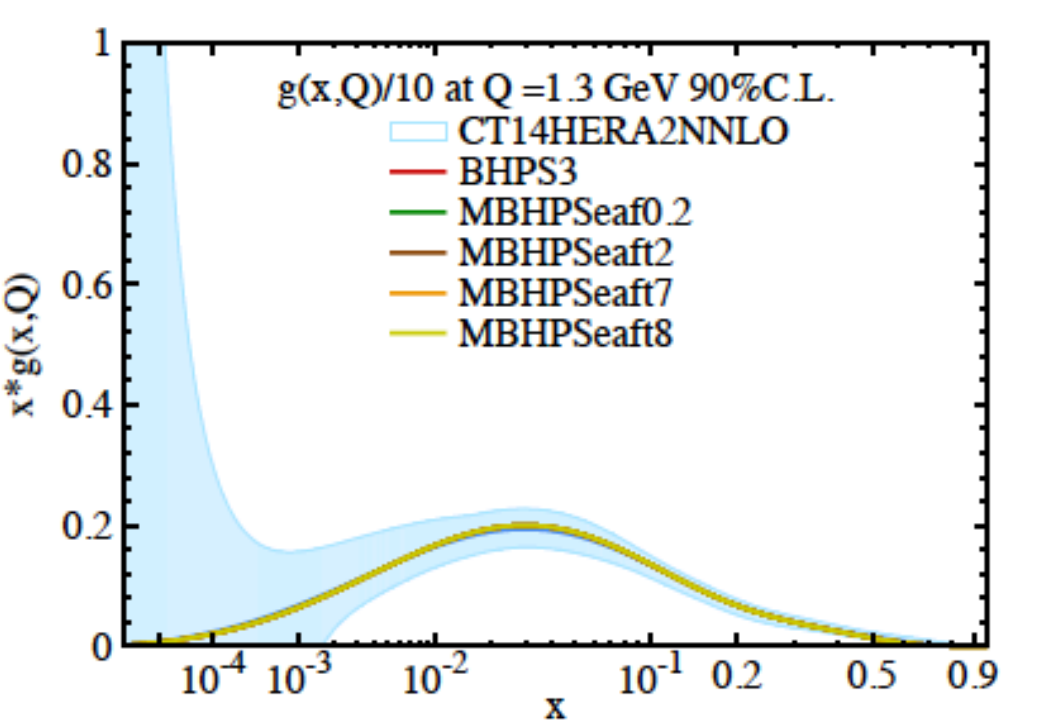
g(x,Q)/10 at Q =1.3 GeV 90%C.L.
CT14HERA2NNLO
BHPS3
MBHPSeaf0.2
MBHPSeaft2
MBHPSeaft7
MBHPSeaft8
x*g(x,Q)
x
1
0.8
0.6
0.4
0.2
0
10^-4
10^-3
10^-2
10^-1
0.2
0.5
0.9

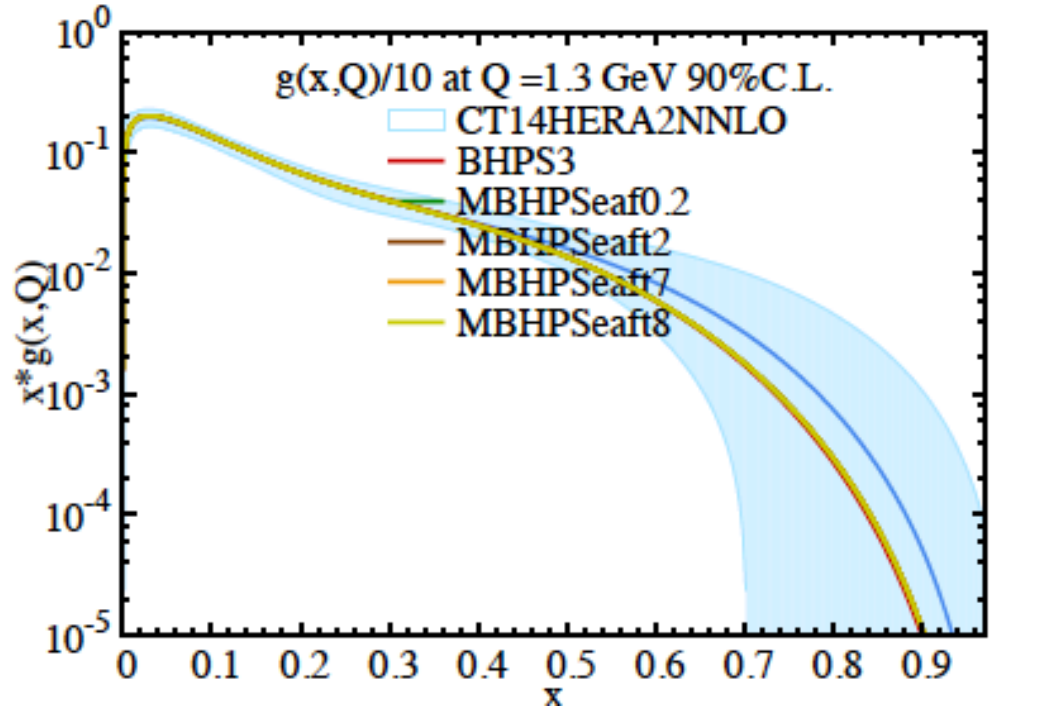
g(x,Q)/10 at Q =1.3 GeV 90%C.L.
CT14HERA2NNLO
BHPS3
MBHPSeaf0.2
MBHPSeaft2
MBHPSeaft7
MBHPSeaft8
x*g(x,Q)
x
10^0
10^-1
10^-2
10^-3
10^-4
10^-5
0
0.1
0.2
0.3
0.4
0.5
0.6
0.7
0.8
0.9

What is intrinsic charm, according to QCD theory?

The ACOT family of schemes are uniquely suited for establishing physical properties of Intrinsic charm:

- The FFN scheme and ACOT schemes are proved by the QCD factorization theorem with explicit power counting of scattering contributions at $p^+ \to \infty$
- Factorization for another GM-VFN scheme (FONLL, TR',…) can be demonstrated, e.g., by reducing to a counterpart ACOT scheme order by order in αs

At $Q^2 \approx m_c^2$ the ACOT Nf =4 scheme reduces to the Nf = 3 scheme, order by order in αs.

In the Nf =3 scheme, (Collins 1998) proved that, at $Q^2 \approx m_c^2$

$$F_2(x,Q^2) = \sum_{a=u,d,s,g} \int_x^1 \frac{dz}{z} C_a\left(\frac{x}{z}, \frac{m_c^2}{Q^2}, \frac{\mu^2}{Q^2}\right) f_a(z,\mu^2) + \mathcal{O}(\Lambda^2)$$

→ Leading power (l.p.)

The l.p. term contains charm propagators only in the coefficient functions, sums only over light-flavor PDFs ➔ In either the Nf=3 scheme or ACOT scheme at $Q^2 \approx m_c^2$ and $\mathcal{O}\left(\alpha_s^n\right)$, the phenomenological IC term is composed of $\mathcal{O}\left(\alpha_s^{n+1}\right)$ l.p. terms and $\mathcal{O}\left(\Lambda^2/m_c^2\right)$ terms

Charm scattering contributions at $Q^2 \approx m_c^2$, sample diagrams

Leading-power charm

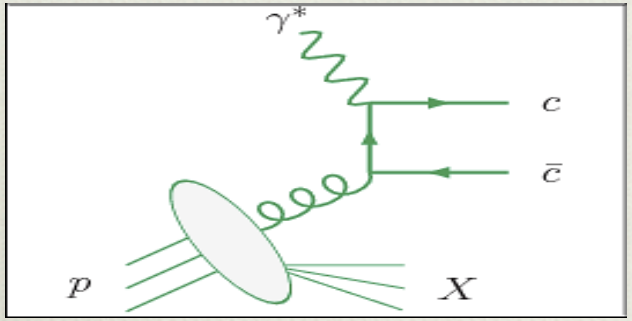

- Single-parton scattering of order $\left(m_c^2/Q^2\right)^k$
- All-order MSbar formalism to factorize into hard scattering cross sections and light parton PDFs
- When matched onto the Nf=4 scheme, **it gives rise to process-independent charm PDF**

Fitted (intrinsic) charm

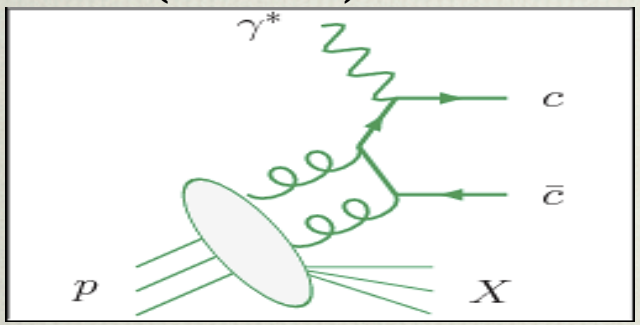

- Multi-parton scattering of order $\left(\Lambda^2/m_c^2\right)^k$
- A power suppressed correction to the factorized cross section.
- Currently not covered by MSbar factorization theorem; ``**IC PDF'' can be process dependent**.

Consequences for interpretation of IC PDFs

The phenomenological IC PDF is a model for $\mathcal{O}\left(\alpha_s^{n+1}\right)$ l.p. and $\mathcal{O}\left(\Lambda^2/m_c^2\right)$ scattering terms. The standard formalism does not tell us how to factorize the IC contributions into hard perturbative and universal nonperturbative parts. Nevertheless, the CT14 NNLO IC PDFs can be used for first estimates of sensitivity of LHC cross sections to charm scattering contributions beyond l.p. QCD. **[If used with caution!]**

In-depth study of CT14 IC fits (T.-J. Hou)

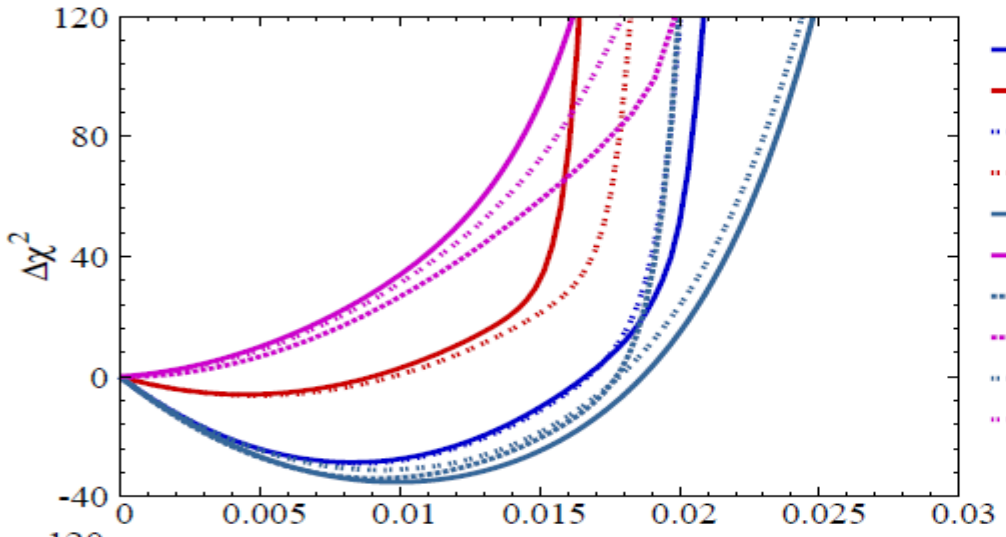

- CT14 BHPS M_C= 1.3 GeV
- CT14 SEA M_C= 1.3 GeV
- CT14(11849) BHPS M_C= 1.3 GeV
- CT14(11849) SEA M_C= 1.3 GeV
- CT14HERA2 BHPS M_C= 1.3 GeV
- CT14HERA2 SEA M_C= 1.3 GeV
- CT14HERA2 BHPS M_C= 1.4 GeV
- CT14HERA2 SEA M_C= 1.4 GeV
- CT14HERA2(11849) BHPS M_C= 1.3 GeV
- CT14HERA2(11849) SEA M_C= 1.3 GeV

11849: Q0=1 GeV, MMHT-like g(x,Q0)

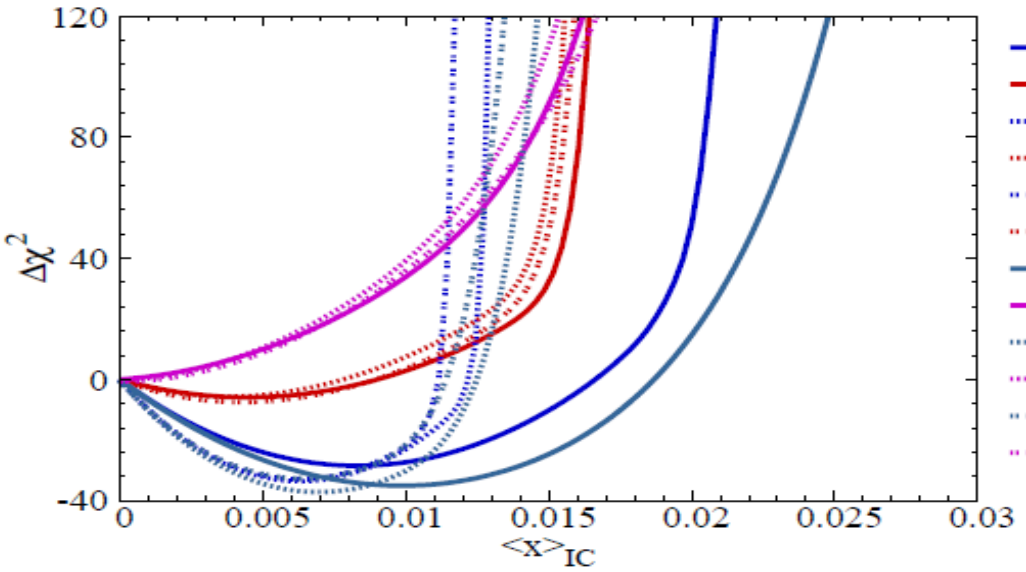

- CT14 BHPS
- CT14 SEA
- CT14, BHPS, w/ EMC
- CT14, SEA, w/ EMC
- CT14(11849), BHPS, w/ EMC
- CT14(11849), SEA, w/ EMC
- CT14HERA2, BHPS
- CT14HERA2, SEA
- CT14HERA2, BHPS, w/ EMC
- CT14HERA2, SEA w/ EMC
- CT14HERA2(11849), BHPS, w/ EMC
- CT14HERA2(11849), SEA, w/ EMC

For the BHPS parametrization, a **marginally** better χ^2 for IC with $\langle x \rangle_{\rm IC}$ ≈1%.
For SEA parametrization, IC with $\langle x \rangle_{\rm IC}$≈1.5% is allowed within uncertainty.

- E866 Drell-Yan dimuon cross section measurement (ID 204)
- Fixed target measurements from BCDMS for F2p and F2d (ID 101, 102)
- ATLAS 7 TeV W/Z cross section measurements (ID 268)
- E605 Drell-Yan fixed target measurements (ID 201)
- The charged current (CC) DIS measurements (ID 110)
- charged-current neutrino interactions on iron CDHSW F2p (ID 108)